IEEE Access
Multidisciplinary | Rapid Review | Open Access Journal

Received August 4, 2019, accepted August 18, 2019, date of publication August 26, 2019, date of current version September 12, 2019.

Digital Object Identifier 10.1109/ACCESS.2019.2937655

A Framework for the Assessment of Distributed Self-Separation Procedures for Air Traffic in Flow Corridors

YONG TIAN[1], (Member, IEEE), YUNLONG DONG[1,2], BOJIA YE[1], AND LILI WAN[1]
[1]College of Civil Aviation, Nanjing University of Aeronautics and Astronautics, Nanjing 210016, China
[2]East China Air Traffic Management Bureau of Civil Aviation Administration of China, Shanghai 201702, China

Corresponding author: Yong Tian (tianyong@nuaa.edu.cn)

This work was supported in part by the National Natural Science Foundation of China under Grant 61671237, and in part by the Natural Science Foundation of Jiangsu Province of China under Grant BK20160798.

ABSTRACT The flow corridor is a tube-shape class of airspace designed for the future air transportation system, which aims to reduce complexity, restructuring the airspace to provide more system capacity. In order to support operational procedures design towards increased operational efficiency in the flow corridor, an accurate assessment of alternative procedures is a pre-requisite. This paper proposes a dynamic stochastic simulation framework including various microscopic behaviors for the assessment of distributed self-separation procedures for the air traffic in flow corridors. We first specify three prominent self-separation modes which distinguish flow corridors from today's airways system, and present detailed self-separation procedures and algorithms in a parallel-lane flow corridor incorporating self-separating, lane-passing and lane-switch behaviors based on the aircraft dynamic model and the proportional derivative control theory. Then, incorporating these self-separation algorithms, a dynamic stochastic simulation modeling framework is constructed to assess and compare the alternative distributed self-separation procedures. The framework is applied to a parallel-lane flow corridor deployed from Beijing nearby airports (ZBAA, ZBTJ and ZBNY) to Guangzhou nearby airports (ZGGG, ZGSZ and ZGSD) in China, and the self-separation procedures were thoroughly assessed with both realistic and simulated data for benefits assessment and sensitivity analysis. Results show that the speed-based operational procedure is more suitable for high-density operations while the other two procedures have more flexibility which can be used for air traffic flow contingency management and/or trajectory management.

INDEX TERMS Airspace design, air transportation, flow corridors, self-separation operations, simulation modeling.

I. INTRODUCTION

In order to enable a substantial increase in airspace capacity to meet future demand for air travel while maintaining safety, many countries and regions are undergoing the air transportation system transformation [1], [2]. The flow corridor is a new airspace design aims to reduce complexity (disorder of air traffic distribution), restructuring the airspace to provide more system capacity, or allocating time-of-arrival and departure slots to runways or airspace [3]. A well designed flow corridor is a long tube of near-parallel Four-Dimensional Trajectory (4DT) assignments for large numbers of separation-capable aircraft traveling in the same direction which consequently achieves a very high traffic throughput, while allowing traffic to shift as necessary to enable more effective weather avoidance or reduce congestion. Three prominent new attributions that would distinguish from today's airways are: allowance for multiple parallel lanes of traffic; capitalization on advanced communication, navigation, and surveillance technology to enable changes in separation, such as self-separation, potentially reduce separation standards within corridor; dynamic activation rules to add or remove corridor structures, as needed, throughout the day [4].

The flow corridor integrates a range of new airspace concepts proposed by researchers, including Dynamic Airspace Super Sectors (DASS) [5], High Volume Tube Shaped Sectors (HTS) [6], Freeways [7], tubes [8], [9], Self-separation

The associate editor coordinating the review of this article and approving it for publication was Haluk Eren.

Corridor (SSC) [10], and Dynamic Multi-track Airways (DMA) [11]. Over the past two decades, previous research has explored the operational concepts, placement of networks and performance evaluation.

The early years of research focused on operational concepts. In 2003, Alipio et al. proposed a kind of one-directional, high density highways in the sky, like thin ribbons of airspace stretching over the sky and connecting major airports, which may decrease Air Traffic Controller (ATC) workload and allow higher densities of aircraft to be safely monitored [5]. In 2004, Yousefi et al. suggested to include parallel lanes to increase the tube's capacity, breakdown lanes to accommodate avionics failures and passing lanes to accommodate aircraft with different performance characteristics [6]. In 2005, Hering presented a geographical layout located in or over the tropopause as a reserved, isolated airspace [7]. The airspace is defined distributed over consecutive flight levels, and only one can be activated for use each time. In 2007, Mundra et al. focused on integrating the Required Navigation Performance (RNP), Automatic Dependent Surveillance-Broadcast (ADS-B), Cockpit Display of Traffic Information (CDTI), and air/ground data communications in the concept to promote the self-separation capability for aircraft [10]. In 2008, Wing et al. considered that dynamic rerouting capability should be incorporated into the concept with consideration of the dynamic and unpredictable nature of weather and congestion every day, and defined a comprehensive operational concept for the flow corridor.

With the mature of operational concept, the geometry and placement of flow corridor network become another research focus. Yousefi et al. performed a statistical analysis of city-pair traffic, and use the velocity vector field methodology to determine the location of potential corridors [4]. Furthermore, they predicted the periods during which corridors should be active, or how their centerline should dynamically change in response to changes in demand profiles and weather disruptions [6]. Sridhar et al. grouped airports into regions and designed a series of tubes connecting major regions to create the corridor network [12], [13]. Both the Weighted-Proximity Classifier (WPC) and the Clustering by Region Growing (CRG) method are used to achieve the grouping for improving the performance of corridor network. Sheth et al. presented a traffic density-based method through recording the count of all aircraft on a 10 nm by 10 nm grid draped over the airspace, and selected the top-50 airport pairs as the start and end points for network construction [14]. Xue and Kopardekar proposed a Hough transform method to cluster great circle trajectories to form the corridor network [15]. Kotecha and Hwang optimized the flow corridor network based on constrained graph method with consideration of the shortest path, distance constraint, angle constraint and entry/exit constraint [16].

In recent decade, the field of performance evaluation has attracted more and more attention. Xue and Zelinski selected a single corridor and presented macroscopic analyses of its spatial and temporal utilization, impact on the remaining traffic and the potential benefit [17], [18]. They also investigated the controller workload, the acceptance of extra fuel or distance, and the complexity reduction in underlying sectors. Yousefi et al. assessed the benefit of corridor network by comparing efficiency gained by joining the corridor network against extra distance traveled to join the network from a macroscopic perspective [4]. Ye et al. built a microscopic model with two parallel lanes which includes the self-separation behavior of aircraft individually in flow corridor, and analyzed the tradeoff between operational risk and capacity [19], [20]. Also, the impact of some different self-separation parameters on capacity and conflicts of the flow corridor were further analyzed. Zhang et al. incorporated the microscopic simulation model and the events leading to actual a near mid-air collision (NMAC), used the dynamic event trees to evaluate the effectiveness of subsequent safety layers that protect against collisions [21]. Some progress has been made with the in-depth study, however, as an important prerequisite for accurate evaluation, which self-separation procedure is the best for aircraft in flow corridor remains unsolved. Although several studies had proposed some distributed self-separation operational procedures concept, no quantitative analysis of the alternative procedures have been well studied with consideration of the aircraft performance and operating model.

In this paper, we develop a simulation modeling framework for the assessment of distributed self-separation operations for the air traffic in flow corridors. We first specify three prominent self-separation modes that would distinguish the flow corridors from today's airways system. Then, a potential parallel-lane flow corridor instance is initialized with realistic data, followed by the design of detailed self-separation procedures and algorithms which incorporate self-separating, lane-passing and lane-switch behaviors based on the aircraft dynamic model and the proportional derivative control theory. The dynamic stochastic simulation framework is proposed and visually verified by google earth, and three alternative self-separation procedures were thoroughly assessed with both realistic and simulated data for benefit assessment and sensitivity analysis.

The main contribution of this research is the simulation-based framework to assess the alternative distributed self-separation procedures, which includes various microscopic self-separated behaviors of aircraft individually for different procedures in the flow corridor. The framework allows us to comprehensively assess different aircraft operations for the air traffic in flow corridors with both realistic and simulated data.

Using the electronic Aeronautical Information Publication (AIP) and Chinese realistic flight operations data between March 26th 2017 and October 28th 2017 from Civil Aviation Administration of China (CAAC), a parallel-lane flow corridor model is deployed between Beijing nearby airports (ZBAA, ZBTJ and ZBNY) and Guangzhou nearby airports (ZGGG, ZGSZ and ZGSD). Three prominent self-separation procedures were thoroughly assessed for the proposed flow corridor with both realistic and simulated data for benefits assessment and sensitivity analysis. The evaluation results are generalizable, because the simulation results reflect some common characters of the traffic operations.

The proposed models may also be applied in real time from both the airspace management aspect and the aircraft operational aspect. From the airspace management aspect, an auxiliary decision system could be developed by incorporating these models to help the air traffic managers to deploy a flow corridor with appropriate self-separation procedures in real time. From the aircraft operational aspect, the proposed models include the basic self-separation rules and procedures can be further used to develop distributed algorithms which can be installed in the cockpits to help aircraft self-separating with each other in the flow corridor in real time.

The rest of the paper is organized as follows: Section II introduces and analyzes the prominent self-separation modes for designing alternative distributed self-separation procedures. Section III presents a parallel-lane flow corridor model and the core parts of the dynamic stochastic simulation modeling framework. Section IV employs numerical simulation and sensitivity analysis to compare alternative distributed self-separation procedures with both realistic and simulated data. Finally, Section V summarizes conclusions and indicates the next research steps.

II. ALTERNATIVE DISTRIBUTED SELF-SEPARATION OPERATIONS IN FLOW CORRIDORS

Current airways are typically single-track, bidirectional and multi-layered structure which are divided into en-route sectors, and the air traffic controllers of the sectors coordinate the movement of aircraft to maintain safe distances between them. However, the self-separation based rules and procedures are proposed in the flow corridor aims to reduce controller workload and increase route capacity. The distributed self-separation capability is one of the prominent attributes that would distinguish flow corridors from today's airways system. It implies that during the operation in pre-defined corridors, the flight crew can use advanced communication, navigation and surveillance technology to monitor and separate themselves from other aircraft, thereby reducing air traffic controllers' workload and increasing their productivity. Currently, within the flow corridors concept, three prominent self-separation modes for the aircraft operation in the flow corridors are the speed-based procedure, speed-independent with passing procedure, and the completely speed-independent procedure.

A. SPEED-BASED OPERATIONAL PROCEDURE

The speed-based operational procedure was initially proposed by Wing et.al [11], which is relatively easy to implement in the flow corridor. In this procedure, flights are supposed to be assigned onto one of the flow corridor lanes closest to their desired cruise Mach number without passing their lead aircraft, as shown in Figure 1. Then, aircraft would always maintain sufficient separation relative to the aircraft ahead of them and fly the lane-specific Mach number for the entire length of the flow corridor. The separation could be measured in either distance or time.

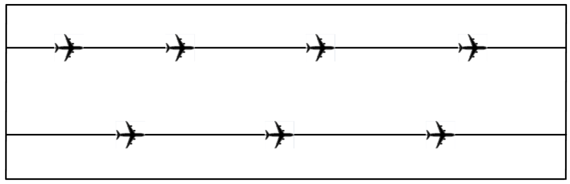

FIGURE 1. Speed-based operational procedure.

Usually, the flow corridor controller is responsible for issuing the trailing aircraft the identity of the lead aircraft and the spacing interval assignment, and the pilot of the trailing aircraft transfers this information to the airborne equipment for self-separation operation. To enhance robustness, a lead aircraft might slow when encountering unexpected influence, and all following aircraft should automatically slow in turn in complying with their self-separation procedure.

For safety consideration, some aircraft are required to fly with a sub-optimal cruise speeds which may limit the benefits achievable from the flow corridor. Mach number assignments for each lane are determined based on the flights demand for the flow corridor at initialization, so as to achieve the optimal performance for the actual fleet mix. In this procedure, optimizing the lane speeds for the most common aircraft types in the participating fleet, increasing the number of lanes in flow corridor, and reducing the fleet diversity supported by the flow corridor should be three primary methods for mitigating the negative effect.

B. SPEED-INDEPENDENT WITH PASSING PROCEDURE

The speed-independent with passing mode was firstly proposed by Alipio *et al.* [5], which is the earliest mode proposed by related researchers. In this procedure, two categories of lanes are defined for aircraft operations which are the nominal lane and passing lane, as shown in Figure 2. Aircraft are assumed to be assigned onto a nominal lane at the beginning with their favorite Mach numbers, but are permitted to shift over to a passing lane to overtake the slower-moving aircraft in front of them.

Once an aircraft enters the nominal lane, the pilot of the trailing aircraft is responsible for identifying the lead aircraft and spacing interval all the time. The distributed algorithm for self-separation operation will determine the triggering condition of passing maneuver by considering the velocities difference, separation variation of related aircraft and the availability of the passing lane etc. The passing maneuver must be accomplished without losing separation with any other aircraft, and the following should automatically slow down to the speed of its lead aircraft to maintain safety if the passing triggering condition cannot be satisfied.

The passing option permits aircraft to remain at their optimal speeds for much of the length of the flow corridor unless the passing lane was unavailable for use. The availability of

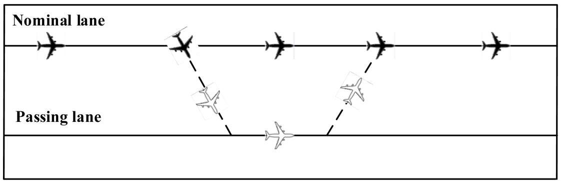

FIGURE 2. Speed-independent with passing procedure.

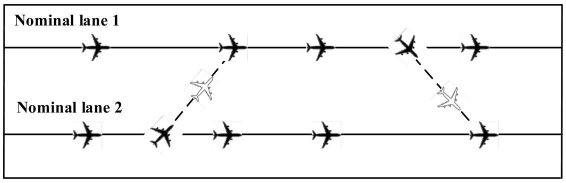

FIGURE 3. Completely speed-independent procedure.

passing lane may limit the benefits achievable from the flow corridor. In this procedure, determining the number of passing lane for each nominal lane, designing an optimal passing trigging condition for the aircraft types in the participating fleet, and designing an appropriate passing maneuver should be three main methods for mitigating the negative effect.

C. COMPLETELY SPEED-INDEPENDENT PROCEDURE

The completely speed-independent mode is a variant of the speed-independent with passing mode that permits aircraft to remain permanently on the passing lane [19], [23], [24]. In this procedure, all lanes are treated as the nominal lanes for each aircraft, as shown in Figure 3. The aircraft are assumed to be assigned onto each lane randomly with their favorite Mach numbers, and may adjust their velocity, separation and switch lane for overtaking or avoiding the loss of the minimum separation as required. This procedure is similar to the ground traffic operations in the highway, but with more complex rules for safety and efficiency consideration.

The distributed algorithm for self-separation operation in this procedure is similar to the speed-independent with passing one. It would determine the triggering condition of lane-switch maneuver by considering the velocities difference, separation variation of related aircraft and the availability of the other lane etc. However, since the other lane is also a nominal lane which may accommodate many aircraft at the same time. Every maneuver in the procedure must be accomplished without any conflict with other aircraft in the flow corridor.

The completely speed-independent procedure increases the movement flexibility extremely for the aircraft operations in the flow corridor. However, the operational risks may limit the benefits achievable from the flow corridor. In this procedure, designing optimal self-separation rules, appropriate lane-switch trigging condition, and good lane-switch maneuver are key points for mitigating the negative effect.

III. SIMULATION SETUP

This section presents a potential parallel-lane flow corridor model, followed by the description of the core parts of the dynamic stochastic simulation modeling framework for assessing the alternative distributed self-separation operations in flow corridor.

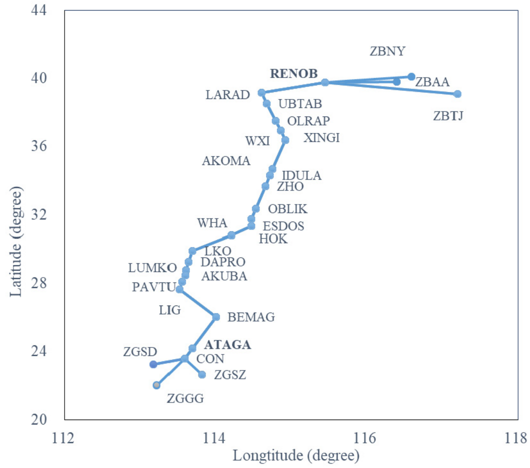

FIGURE 4. Flow corridor design for upper air route from Beijing to Guangzhou.

A. THE FLOW CORRIDOR STRUCTURE INITIALIZATION

Although the assessment framework proposed in this paper can be applied to other corridor models, without loss of generality, a potential flow corridor instance is designed with realistic operating data for simulation modeling. The basic data for this work were obtained from the Civil Aviation Administration of China's electronic AIP data and realistic flight operations data.

After initial analysis of the current air route structure and traffic demand, we chose the city-pair between Beijing and Guangzhou as the flow corridor design basis. It's one of the busiest air routes in China and potentially suitable for the deployment of flow corridor. The upper air route A461 for this city-pair links the Beijing Capital International Airport (ZBAA), Tianjin Binhai International Airport (ZBTJ) and Beijing Nanyuan Airport (ZBNY) around Beijing city, to the Guangzhou Baiyun International Airport (ZGGG), Shenzhen Bao'an International Airport (ZGSZ) and Zhuhai Jinwan Airport (ZGSD) around Guangzhou city, serving more than 200 flights each day and 486 million passengers in 2017.

The tradition upper air route between Beijing and Guangzhou is 970 nm long with more than 20 navigation stations which is in fact also a RNAV route with the same route structure in China, as shown in Figure 4. For easy of deployment and comparison with realistic data, we collocate the flow corridor with the existing airway structure with specification entry point (RENOB) and exit point (ATAGA). For the geometry, the high altitude RNAV Q-routes are used as a basis for the flow corridor design [4]. The structure is designed to be two closely parallel lanes with the centerlines 8 nm apart located at the Flight Level 350. The total wide of the corridor is set as 16 nm, and the centerlines are supposed to be laterally separated by 4 nm and are vertically separated by 1,000 ft with the flow corridor boundaries.

TABLE 1. Standard atmospheric for flow corridor on FL350.

Level (ft)	Temperature (C°)	Pressure (hPa)	Density (kg.m^{-3})	Speed of sound (knots)
35000	-54.3	238	0.3796	576

The flow corridor access is limited to the aircraft equipped with advanced navigation equipment and data links such as Airborne Separation Assurance System (ASAS), ADS-B and CDTI, but the unknown failure of the equipment is not considered in the research [20], [23]. The International Standard Atmosphere (ISA) is assumed on the flow corridor flight level which implies that the density, pressure and temperature magnitudes are functions of the altitude [25], as shown in Table 1.

B. SIMULATION MODELING FOR SELF-SEPARATION PROCEDURES

To simulate the distributed self-separation procedures with microscopic behaviors in the flow corridor, the self-separating, lane passing and switch behaviors models are introduced in this section with the core algorithms for alternative procedures. We used the real flights information including the aircraft types, time interval and volume of aircraft to improve the fidelity of the simulation model.

1) SELF-SEPARATING WITH LEAD AIRCRAFT

In this paper, the dynamics of aircraft from the point view of ATC are expressed by the following set of non-linear Ordinary Differential Equations (ODE) from Glover and Lygeros [26] as equations (1). The basic state of the model is the horizontal position (x and y) and altitude (h) of the aircraft, the true airspeed (v), the flight path angle (γ) and the heading angle (ψ). The control inputs to the model are the engine thrust (T), the angle of attack (α) and the bank angle (ϕ). The movement of the aircraft is also affected by the wind which acts as a disturbance. We ignored the effect of the wind, spoilers, and leading edge slats, etc. in the simulation.

$$\begin{cases} \dot{x} = v\cos(\psi)\cos(\gamma) \\ \dot{y} = v\sin(\psi)\cos(\gamma) \\ \dot{h} = v\sin(\gamma) \\ \dot{v} = \dfrac{1}{m}[T\cos(\alpha) - D - mg\sin(\gamma)] \\ \dot{\psi} = \dfrac{1}{mv}[L + T\sin(\alpha)]\sin(\phi) \\ \dot{r} = \dfrac{1}{mv}[(L + T\sin\alpha)\cos\phi - mg\cos\gamma] \end{cases} \tag{1}$$

m is the mass of the aircraft and g is the gravitational acceleration. L and D denote the lift and drag forces respectively, which are the functions of the state and angle of attack as follows equations:

$$L = \frac{C_L S\rho}{2}(1 + c\alpha)v^2 \tag{2}$$

$$D = \frac{C_D S\rho}{2}(1 + b_1\alpha + b_2\alpha)v^2 \tag{3}$$

where S is the surface area of the wings, ρ is the air density (which depends on altitude), and C_D, C_L, c, b_1 and b_2 are aerodynamic lift and drag coefficients whose values generally depend on the phase of the fight. All aerodynamic and engine aircraft characteristic functions are obtained from Base of Aircraft Data (BADA)created by European Organization for the Safety of Air Navigation (EUROCONTROL) in cooperation with aircraft manufacturers and operating airlines [26].

The self-separation behavior is adapted by the following non-linear differential equations. A proportional derivative (PD) controller is used for calculating the acceleration of aircraft as equation (4), which can help the pilot to self-separate with its lead aircraft with consideration of the aircraft type, velocity difference, separation variation trend and time-lag etc.

$$\ddot{x}_i(t) = \tau_1(x_{i-1}(t - t_{lag}) - x_i(t - t_{lag}) - s_{\min} - s_b) + \tau_2(\dot{x}_{i-1}(t - t_{lag}) - \dot{x}_i(t - t_{lag})) \tag{4}$$

where $\ddot{x}_i$ represents the acceleration of aircraft i at simulation time t, $x_i(t)$ and $\dot{x}_i(t)$ are the longitudinal position and velocity of aircraft i at simulation time t, t_{lag} represents the time lag for aircraft which refers to the flight technical tolerances, $s_{\min}$ and s_b are the *minimum separation* and *separation buffer* for the aircraft self-separated with lead one in the flow corridor, $\dot{x}_{i-1}(t - t_{tag})$ represents the velocity of lead aircraft $i - 1$ at the simulation time t-t_{lag}, τ_1 and τ_2 are two tuning parameters used for keeping the target aircraft within the appropriate separation and velocity limits. In general, the equation shows that the acceleration of the aircraft is a function of the *current separation, minimum separation, separation buffer, velocity difference and time lag* etc. Also, the aircraft position and velocity will be updated along with the simulation time following the dynamic model introduced in equations (1)-(3). ODEs (1)-(4) can be computed by Laplace transform.

2) LANE PASSING AND SWITCH BEHAVIORS

Lane passing and switch behaviors are two prominent abilities which can increase the flexibility for the aircraft flying in the flow corridor. The main difference between two behaviors is that the lane switch behavior is designed for the completely speed-independent procedure which permits the aircraft to remain permanently on the new lane.

In our simulation model, if the lane-switch trigger conditions are satisfied, the target aircraft in both behaviors are supposed to flies a 30° (θ) path to another lane with their desired cruise Mach number while the aircraft in lane-passing behavior will keep on trying to return to the original lane after the surpassing, as shown in Figure 5(a).

The lane-switch trigger conditions for the speed-independent with passing procedure are defined as follows: (a) the separation with the lead aircraft is less than *distance threshold* (s_{thr}); (b) the velocity difference with the lead aircraft is larger than some *velocity difference threshold* (v_{thr}); (c) make a projection for the planned passing aircraft onto another lane (30° path) to find its new lead and/or trailing

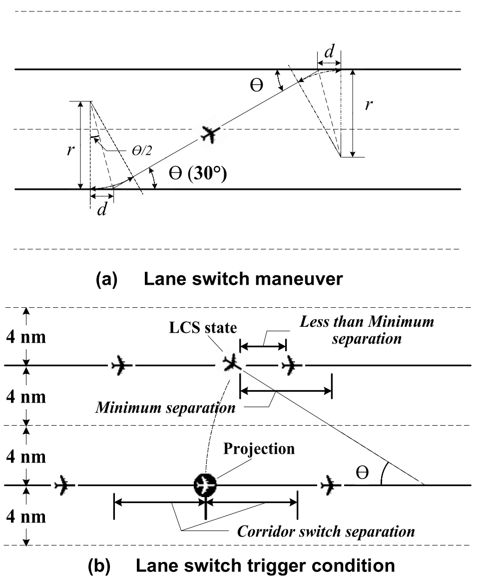

FIGURE 5. Lane switch trigger conditions and lane switch behavior.

aircraft in that lane (if they exist), both of the separations between the potential lane-passing aircraft and the new lead and trailing aircraft must be larger than the *distance threshold* or there is no new lead and/or trailing aircraft in the new lane, as shown in Figure 5(b). The projection position of aircraft can be calculated based on its along-track position, the two lane center distance, and the turning angle based on trigonometric function.

For the passing aircraft that desired to return to its original lane, one more condition need to be satisfied is that the velocity difference between the returning aircraft and its new lead aircraft must be less than the *velocity difference threshold* defined above. This condition is for safety and efficiency consideration, which can prevent aircraft consecutively switching lane.

3) ALGORITHM FOR DISTRIBUTED SELF-SEPARATION PROCEDURES

Based on the microscopic behaviors introduced above, we develop the algorithms for alternative distributed self-separation procedures. For the speed-based procedure, we develop the framework of aircraft flying at the parallel-lane flow corridor in **algorithm 1**. Each aircraft initially enters one of the flow corridor lanes with specific type and states including the initial velocity, separation, acceleration etc. Then the self-separation algorithm begins and all aircraft states are updated along with the simulation time according to the proposed dynamics model until all aircraft finish flying in all lanes.

For the speed-independent with passing procedure, a distributed self-separation algorithm with lane passing behavior is developed as illustrated in **algorithm 2**. Each aircraft initially enters the nominal lane in the flow corridor and flies at their desired cruise Mach number. Some aircraft will try to passing its lead aircraft with the help of passing lane if the lane-switch trigger conditions are satisfied, while the other aircraft try to self-separate with their lead ones. All aircraft states are updated along with simulation time according to the proposed dynamics model and lane passing behavior until all aircraft finish flying in the flow corridor.

For the completely speed-independent procedure, a distributed self-separation algorithm with lane switch behavior is developed as illustrated in algorithm 3. Each aircraft initially enters one of the flow corridor lanes and flies at their desired cruise Mach number. Some aircraft will try to switch the lanes if the lane-switch trigger conditions are satisfied, while the others try to self-separate with their lead ones. All aircraft states are updated along with simulation time according to the proposed dynamics model and lane switch behavior until all aircraft finish flying in the flow corridor.

Based on the core models and algorithms introduced above, we developed a dynamic stochastic simulation modeling framework which is written in the C++ language and visually verified by google earth for assessing the alternative distributed self-separation operations in flow

Algorithm 1 Framework of Speed-Based Operational Procedure

```
Initialize aircraft type and states for each aircraft in the lanes of flow corridor
loop while not all aircraft finish flying in the lanes
    Update aircraft states in the lanes
    if current separation < distance threshold then
        Self-separating with the lead aircraft
    else
        Flying at the lane-specific cruise Mach number
end of loop
```

Algorithm 2 Framework of Speed-Independent With Passing Procedure

```
Initialize aircraft type and states for each aircraft in the lanes of flow corridor
loop while not all aircraft finish flying in the lanes
    Update aircraft states in the lanes
    if lane-switch trigger conditions are satisfied then
        Switch to passing lane
        if lane return conditions are satisfied then
            Flying back to nominal lane
        else
            Flying at the passing lane with desired cruise Mach number
    else
        Flying at the nominal lane
            if current separation < distance threshold then
                Self-separating with the lead aircraft
            else
                Flying at the desired cruise Mach number
end of loop
```

Algorithm 3 Framework of Completely Speed-Independent Procedure

Initialize aircraft type and states for each aircraft in the lanes of flow corridor
loop while not all aircraft finish flying in the lanes
  Update aircraft states in the lanes
  if lane-switch trigger conditions are satisfied **then**
    Switch to the other nominal lane
  else
    Flying at the current nominal lane
    if current separation $<$ distance threshold **then**
      Self-separating with the lead aircraft
    else
      Flying at the desired cruise Mach number
end of loop

corridor. The simulation framework extends the work done in Ye *et al.* [19], [20] by incorporating different distributed self-separation operations for assessment and comparison. Some more simulation details can be found in previous work.

IV. NUMERICAL TEST

This section employs a numerical test by using the proposed dynamic stochastic simulation framework for assessing and comparing distributed self-separation procedures with both realistic and simulated data.

A. DATA PRE-PROCESS AND SIMULATION INITIALIZATION

The dataset used for the numerical test includes all Chinese domestic flights flying the A461 route from airway point RENOB to ATAGA between March 26th 2017 and October 28th, 2017, inclusive. There are altogether 20,434 flights flying from the Beijing nearby airports (ZBAA, ZBTJ and ZBNY) to the Guangzhou nearby airports (ZGGG, ZGSZ, and ZGSD). We focus our initial analysis on the number of flights and cruise time (from RENOB to ATAGA) for different weekdays during the investigated time period in order to capture the performance of the conventional procedure as the baseline and to initialize some simulation parameters.

Figure 6 compares the number of flights and the realistic cruise time for different weekday using box plots. The box extends from the lower to upper quartile values of the data, with a line at the median. The whiskers extend from the box to show the range of the data. Flier points are those past the end of the whiskers.

We see that in general the number of flights on Thursday are more than other weekdays with the median value of 101 as shown in Figure 6(a). The medians of cruise time for different weekdays remain around 130 minutes as shown in Figure 6(b). A noteworthy point is that there are many flier points in the figure which implies that the flights were often suffered serious delays in this route.

Also, we report the en-route flying time across aircraft types in Table 2, including the aircraft type, number of flights, percentage, minimum, mean, maximum flying time and the standard deviation in minutes. There are mainly 8 types of aircraft flying in this route, among which the B737 accounts for 8257 flights with the maximum ratio of 43%. The average flying time for different aircraft ranges from 122.51 to 131.84 minutes with about 8 minutes standard deviation.

Figure 7 compares the realistic number of flights for different hour of day using box plots. We can see the operational hours between 7 and 18 are the rush time with more than 5 flights on average entering the route every hour. These periods are selected as the research basis for sensitivity analysis.

We fit the interval arrival distribution and estimate the parameters for the aircraft entering the high altitude en-route during the busy hours, the exponential distribution with a mean of 10.57 minutes is fitted as the appropriate distribution for aircraft interval arrival in the busy hours, which is used as the basis for simulation parameters initialization.

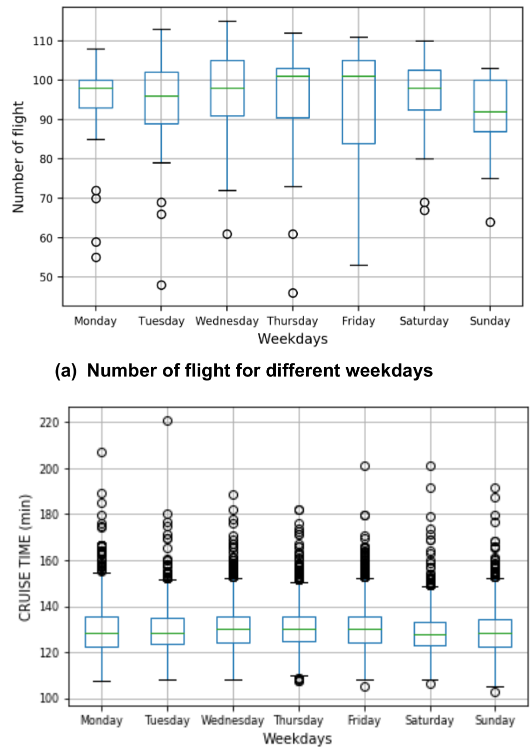

(a) Number of flight for different weekdays

(b) Cruise time for different weekdays

FIGURE 6. Realistic flying data analysis for different weekdays.

TABLE 2. En-route flying time between Beijing and Guangzhou.

Aircraft type	Number of aircraft	Flying time (min)			
		Min	Max	Mean	Standard Deviation
A320	3626	108.84	220.73	131.84	8.86
A332	1055	108.08	165.17	128.35	7.88
A333	3156	109.6	200.94	129.08	8.52
A388	404	106.56	161.36	122.70	7.30
B737	8257	105.04	207.03	131.08	8.61
B772	465	105.04	164.41	126.09	7.89
B77W	1096	108.84	168.97	128.58	8.08
B787	1338	102.75	180.39	122.51	7.87

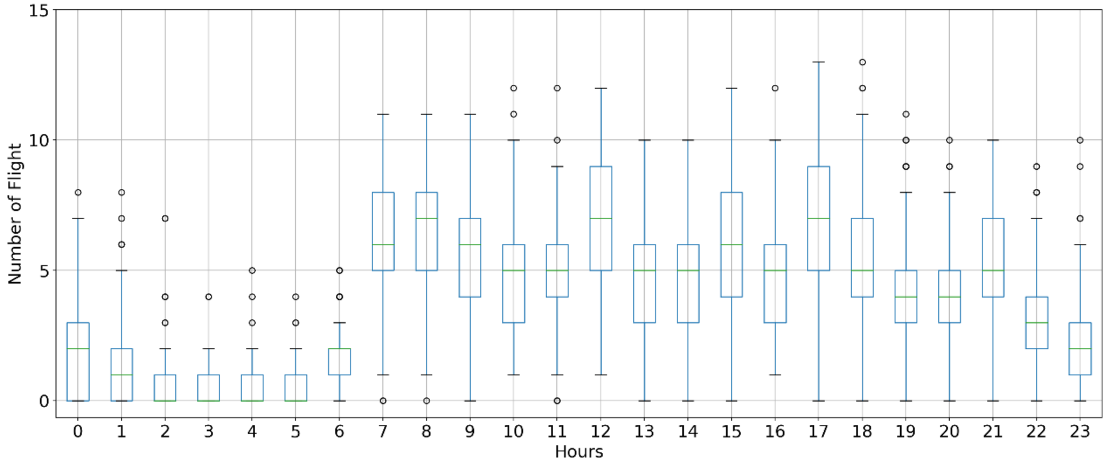

FIGURE 7. The realistic number of flights for different hour of day.

TABLE 3. Example supply parameters.

Parameters	Value	Parameters	Value
Simulation time-step	6 s	Simulation times	20 times
Corridor length	970 nm	Aircraft number	20,000
Minimum separation	5 nm	Time lag	6 s
Separation buffer	2 nm	Tuning parameter 1	0.2
Distance threshold	10 nm	Tuning parameter 2	0.8
Velocity difference threshold	40 nm	Interval arrival	EXP (10.57) min
Lane switch angle	30°	Fleet mix	Realistic proportion

The aircraft performance parameters used in this research come from the User Manual for BADA published by EUROCONTROL, including aircraft type, mass, wing surface area, the reference mass, the maximum operational Mach number, standard cruise Mach number above Mach transition altitude, maximum longitudinal acceleration for civil flights, engine thrust parameters, fuel flow parameters etc. Some important simulation parameters and self-separation procedures variables in the numerical test are shown in Table 3. The simulation times, aircraft number, interval arrival and fleet mix are used for sensitivity analysis specifically.

B. OPERATIONAL DAY BENEFITS ASSESSMENT

We first conduct the operational day benefits assessment with realistic data. One week data between July 17th and July 23th in 2017 was selected, and three alternative procedures including the speed-based operational procedure (P_1), the speed-independent with the passing procedure (P_2) and the completely speed-independent procedure (P_3) were assessed in the simulation. The expected flying time was used as the operational metric for benefits comparison.

Table 4 illustrates the expected flying time of the flight in the testing day for different self-separation procedures. The minimum, maximum and expected flying time with standard deviation were selected as metrics for different procedures comparison. Also, the flying time variation with the realistic data was calculated in the last column of the table.

Overall, all three procedures achieved some improvement in flying time with an average of 2.61 minutes reduction, but no procedure had a distinct advantage in this aspect. The completely speed-independent procedure (P3) showed better performance in the minimum flying time than the other two while all three procedures had almost the same maximum flying time. The optimal procedure changed with the testing day in the mean of flying time while the speed-based operational procedure (P1) kept stable standard deviation all through the week. It is hard to determine which procedure is the best by flying time with current traffic demand.

Also, we analyzed the flying time from the aircraft type aspect to observe the data. Table 5 illustrates the expected flying time and the time difference for alternative self-separation operational procedures with realistic data for all 8 types of aircraft. All aircraft types are showed in the first column of the table.

From Table 5 we can see that all procedures have less expected flying time than the realistic data for all aircraft types, but different aircraft type obtained difference benefits. The expected flying time reductions range from 1.49 minutes to 7.18 minutes across different procedures compared with the realistic data.

Generally, no procedure has a distinct advantage in reducing the flying time for all types of aircraft. But a noteworthy point is that the speed-based operational procedure (P_1) shows an obvious advantage in reducing the flying time for the aircraft closest to the lane-specific Mach numbers than others. Both the speed-independent with the passing procedure (P_2) and the completely speed-independent procedure (P_3) seem do not have this characteristic.

C. SENSITIVITY ANALYSIS FOR DIFFERENT TRAFFIC DEMAND

We conducted a sensitivity analysis for different traffic demand to assess alternative distributed self-separation

TABLE 4. Expected flying time of the flight in the testing day.

Testing Day	Self-separation procedures	Expected Flying time (min) Min	Max	Mean	SD	Mean of realistic flying time (min)	Flying time Variation (min)
Monday 17/07/2017	P_1	123.0	129.4	127.12	3.01	129.39	-2.27
	P_2	118.8	129.4	126.91	3.42	129.39	-2.48
	P_3	118.7	129.4	126.96	3.46	129.39	-2.43
Tuesday 18/07/2017	P_1	123.0	129.3	127.09	3.02	129.50	-2.41
	P_2	118.7	129.4	127.17	3.61	129.50	-2.33
	P_3	118.7	129.4	127.16	3.58	129.50	-2.34
Wednesday 19/07/2017	P_1	123.0	129.4	127.14	3.01	130.40	-3.26
	P_2	118.6	129.4	127.10	3.55	130.40	-3.30
	P_3	118.6	129.4	126.98	3.66	130.40	-3.42
Thursday 20/07/2017	P_1	123.0	129.4	126.87	3.09	130.36	-3.49
	P_2	118.7	129.4	126.99	3.60	130.36	-3.37
	P_3	118.7	129.4	126.85	3.74	130.36	-3.51
Friday 21/07/2017	P_1	123.0	129.3	127.35	2.93	130.19	-2.84
	P_2	118.8	129.4	126.98	3.78	130.19	-3.21
	P_3	118.7	129.4	126.75	3.89	130.19	-3.44
Saturday 22/07/2017	P_1	123.0	129.3	126.90	2.92	128.40	-1.50
	P_2	118.7	129.4	127.37	3.41	128.40	-1.03
	P_3	118.7	129.4	127.08	3.60	128.40	-1.32
Sunday 23/07/2017	P_1	123.0	129.3	126.90	3.08	128.94	-2.04
	P_2	118.7	129.4	126.39	3.97	128.94	-2.55
	P_3	118.6	129.4	126.69	3.83	128.94	-2.25

TABLE 5. Expected flying time and the time difference for alternative self-separation operational procedures.

Aircraft type	Realistic (min)	P1 (min)		P2 (min)		P3 (min)	
	Mean	Mean	Variation	Mean	Variation	Mean	Variation
A320	133.98	129.30	-4.68	129.40	-4.59	129.39	-4.59
A332	130.42	123.01	-7.42	123.75	-6.68	123.28	-7.14
A333	131.17	123.01	-8.16	123.99	-7.18	123.47	-7.70
A380	124.69	123.00	-1.69	119.57	-5.12	119.43	-5.25
B737	133.20	129.30	-3.90	129.30	-3.90	129.34	-3.86
B772	130.67	123.00	-7.67	124.61	-6.06	123.59	-7.08
B77W	128.14	123.00	-5.14	122.42	-5.72	122.31	-5.83
B787	124.50	123.01	-1.49	119.05	-5.45	119.20	-5.30

TABLE 6. The operational metrics data with the increase of traffic volume in 12 busy hours.

Testing Volume	Self-separation procedures	Operational Metric: Expected Flying time (min)	Cumulated delay time (min)	Total fuel consumption(kg)	Pass rate
1X	P1	126.87	59.16	574,879	1.0000
	P2	126.69	47.11	573,839	0.9994
	P3	126.38	25.62	571,676	0.9996
2X	P1	126.87	118.75	1,149,767	1.0000
	P2	127.02	139.14	1,153,196	0.9972
	P3	126.71	95.95	1,147,795	0.9992
4X	P1	126.87	237.44	2,299,528	1.0000
	P2	127.32	358.05	2,311,013	0.9912
	P3	127.13	306.74	2,312,362	0.9984
8X	P1	126.87	475.39	4,599,075	1.0000
	P2	127.37	746.30	4,675,626	0.9879
	P3	127.52	828.21	4,669,103	0.9994

procedures in this section by Monte Carlo simulation. The aircraft types, interval arrivals, and the aircraft accelerations are considered as random variables in the experiments. The aircraft type is generated based on the empirical distribution of realistic data (Realistic percentage of aircraft types, A320: 19%, A332: 5%, A333: 16%, A388: 2%, B737: 43%, B772: 2%, B77W: 6%, B787: 7%). We fitted the interval arrival with the exponential distribution with the mean of 10.57 minutes, and we changed the mean value of interval arrival to generate 2, 4 and 8 times of traffic volume. Also, we add

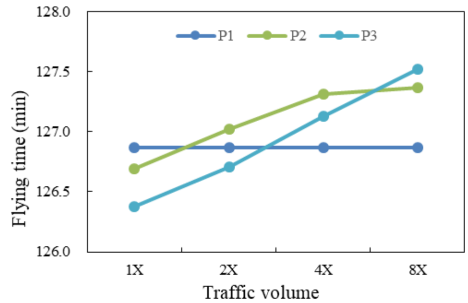

(a) Flying time change trends for three procedures

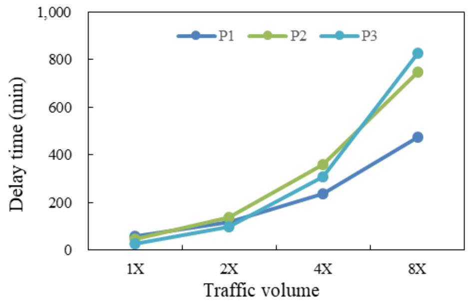

(b) Delayed time change trends for three procedures

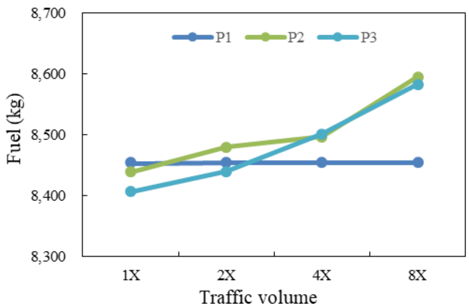

(c) Fuel consumption change trends for three procedures

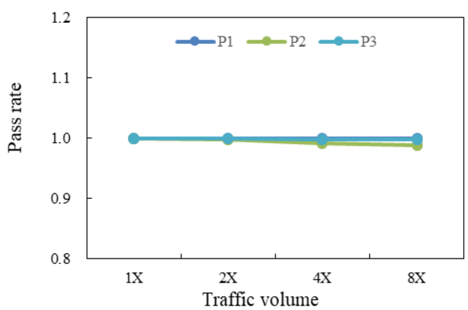

(d) Pass rate change trends for three procedures

FIGURE 8. The operational metrics change trends with traffic volume in 12 busy hours.

some noise follows the normal distribution with zero mean and 0.06 standard deviation to the acceleration to simulate the wind affects.

In addition, the operational metrics including the expected flying time, expected delayed time, cumulated delay time, the total fuel consumption and passing rate were selected for results analysis in the experiments. Specifically, the passing rate represents the percentage of aircraft finish the flight

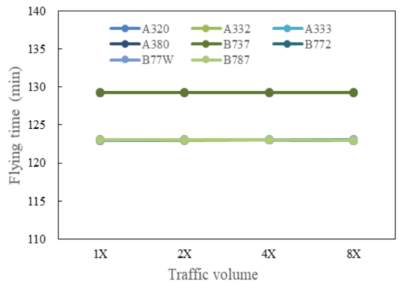

(a) Procedure P1

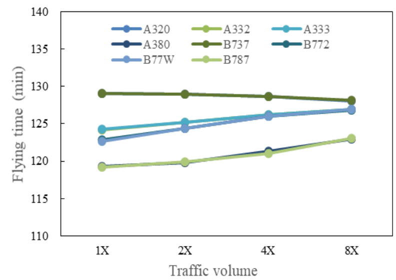

(b) Procedure P2

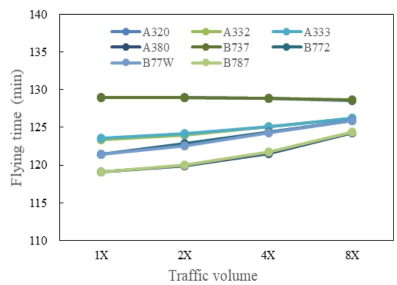

(c) Procedure P3

FIGURE 9. Flying time comparison for alternative procedures with different aircraft types.

plan without loss of the minimum separation within the flow corridor in the simulation. The operational metrics of expected flying time, accumulated delayed time, fuel consumption and pass rate change with 1, 2, 4 and 8 times of the traffic volume in 12 busy hours are shown in Table 6. Also, we plotted the data with broken lines as shown in Figure 8, where three alternative procedures were drawn with different colors respectively. (The traffic volume is obtained through modifying the expected value of the aircraft interval arrival distribution introduced in IV.A).

For the flying time in Figure 8(a), the P1 stay constant with the assumption of no extra wind and other stochastic noise exists in the simulation while the flying time of both P2 and P3 increase with the traffic demand. These trends seem to implicate that P1 has some advantage with the high density volume than the other two procedures, and similar trends can be also found in Figure 8(b) and Figure 8(c). However, a noticeable point is that the P3 shows some advantage when the traffic volume is about twice of the busy hour. Figure 8(d) shows the pass rate changes with the traffic volume, which implies some flights may breakout from the flow corridor with the increase of the traffic volume in P2.

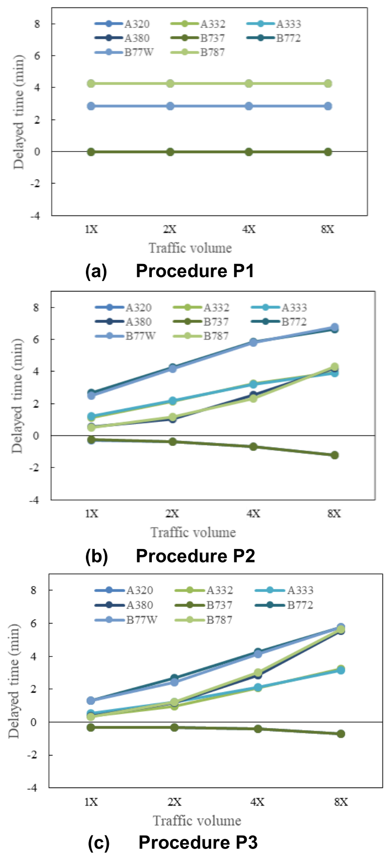

FIGURE 10. Delayed time comparison for alternative procedures with different aircraft types.

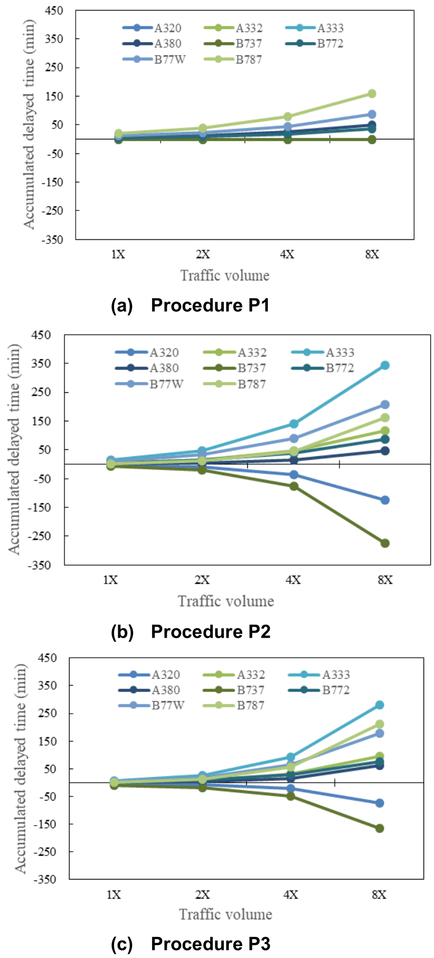

FIGURE 11. Accumulated delayed time comparison for alternative procedures with different aircraft types.

In summary, when the air traffic volume is less than or equal to 2 times of current volume, the procedure P3 shows some advantage over others while the procedure P1 shows more obvious advantages in improving the benefits with the increase of traffic volume in the flow corridor. Compared to P3, the procedure P2 is a less efficiency self-separation procedure, and can only show some advantages over P1 at the current traffic demand.

Also, we compared the operational metrics from the aircraft type aspect. Different from the overall perspective, the expected flying time, delayed time, accumulated delayed time and fuel consumption were selected as the metrics change with 1, 2, 4 and 8 times of the traffic volume in 12 hours. Three alternative procedures are plotted in three different sub-figures while different aircraft types are drawn with different colors respectively. (The traffic volume is obtained through modifying the mean value of the aircraft interval arrival distribution introduced in IV.A).

For the flying time, we can see that there are two parallel broken lines in Figure 9(a) which imply that all aircraft were assigned onto one of the flow corridor lanes closest to their desired cruise Mach number without passing their lead aircraft. Figure 9(b) and Figure 9(c) show similar convergence trends, but P2 seems to converge into one point while P3 seems to converge into two points. This difference should be caused by using different procedures in which P2 only uses one lane as the nominal lane while P3 uses both lanes as the same. Figure 9(b) and Figure 9(c) also imply that although some aircraft with slow cruise Mach number (e.g. B737) reduced the flying time with the increase of the traffic volume, some faster aircraft (e.g. A333, B77W and B787) seem to have slowed down affected by the high-density traffic.

For the average delayed time, we can see that there are three parallel broken lines in Figure 10(a) which imply that there are four desired cruise Mach number for the aircraft in P1. The aircraft flying with their desired cruise Mach number (A320, A332, A333 and B737) in the parallel-lane had no delay time while the aircraft types B772 and B77W encounter an average of 2.85 minutes delays, the aircraft types A380 and B787 encounter an average of 4.27 minutes delays. Figure 10(b) and Figure 10(c) show some interesting divergence trends which imply some aircraft (A320 and B737) may save some flying time while the others may encounter more expected delay as the increase of traffic volume. A noteworthy point is that the divergence trend of expected delayed time in P2 is more obviously than that in P3.

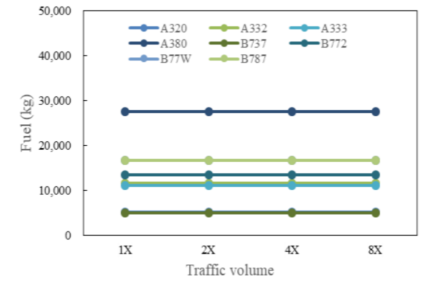

(a) Procedure P1

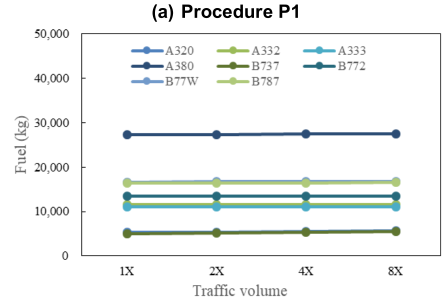

(b) Procedure P2

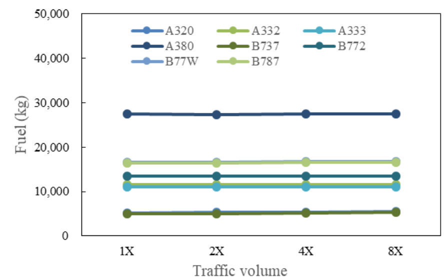

(c) Procedure P3

FIGURE 12. Fuel consumption comparison for alternative procedures with different aircraft types.

The accumulated delayed time takes the number of aircraft into consideration with the average delayed time. In general, the accumulated delay of aircraft in P1 show some slow growth with the increase of traffic volume, and the aircraft flying with their desired cruise Mach number encountered no delays as shown in Figure 11(a). However, in Figure 11(b) and Figure 12(c), P2 and P3 procedures show some obvious divergence trends with the increase of the traffic volume. A320 and B737 saved a large amount of nominal flying time while the others encountered much of growth delays with the increase of traffic volume. Also, the divergence trend of expected accumulated delayed time in P2 is more apparent than that in P3.

For the average fuel consumption in the flow corridor, different type of aircraft has different expected fuel consumption. In generally, the average fuel consumption of aircraft in P1 stay constant with the increase of traffic volume as shown in Figure 12(a) while more fuel was consumed for the aircraft in P2 and P3 due to the dynamic adjustment of the velocities as shown in Figure 12(b) and Figure12(c). A320, A380, B737, and B787 are four aircraft types which have obvious fuel consumption difference in the simulation. Compared to the aircraft in P1, the aircraft A320 in P2 and P3 consumed extra 148.66 kg and 89.98 kg fuel with the original traffic volume, and 579.82 kg and 362.96 kg with 8 times traffic volume, respectively. Also, the aircraft B737 had similar changing trends with A320. However, for the aircraft A380 in P2 and P3, the expected fuel consumption was 179.07 kg and 146.02 kg less than those consumed in P1 with the original traffic volume, and these values reduced to 91.15 kg and 52.32 kg respectively when the traffic volume increased to 8 times. The aircraft B737 had similar changing trends with A380.

In summary, the procedure P1 show more stable performance than other the two procedures in the simulation. P2 and P3 are two similar procedures which try to speed up the aircraft with low cruise Mach numbers and slow down the aircraft with high cruise Mach numbers. The key drawback is that as the aircraft deviated from their desired cruise Mach numbers, some extra fuel will be consumed for dynamic changing of velocities with time. For routine flying without consideration of capacity constraints, P1 is a more preferable procedure. However, P2 and P3 have more flexibility in adjusting aircraft flying time and delay which may be more suitable for the air traffic flow contingency management and trajectory management.

V. CONCLUSION

This paper proposes a simulation modeling framework through which we can assess and compare alternative distributed self-separation procedures for air traffic in the flow corridor. We specify three prominent self-separation modes which would distinguish flow corridors from today's airways system, and present detailed self-separation procedures and algorithms in a parallel-lane flow corridor incorporating self-separating, lane-passing and lane-switch behaviors based on the aircraft dynamic model and the proportional derivative control theory. Building on the self-separation algorithms, a dynamic stochastic simulation modeling framework is constructed to assess and compare the distributed self-separation procedures. Numerical examples illustrate the realistic situations where a parallel-lane flow corridor is deployed between Beijing and Guangzhou in China, and all procedures were thoroughly assessed with realistic data and simulated data for benefit assessment and sensitivity analysis.

Results suggest that all three procedures could achieve some improvement than the current procedure in flying time with an average of 2.61 minutes reduction, but no procedure has a distinct advantage over others. It is hard to determine which procedure is the best by flying time with current traffic demand. From the aircraft type aspect, the speed-based operational procedure shows an obvious advantage in reducing flying time for the aircraft closest to the lane-specific Mach numbers than others while the other two do not have this characteristic.

However, when we increased the air traffic demand from current traffic volume to eight times for sensitivity analysis, some obvious difference appeared in the metrics of the expected flying time, delayed time, accumulated delayed time, pass rate and fuel consumption. A key finding of this research is that the completely speed-independent procedure shows obvious advantage over others when traffic demand is not too high (less than or equal to two times volume in our numerical test), while the speed-based operational procedure instead of its place with the increase of traffic volume (four and eight times volume). The speed-independent with passing procedure is a less efficiency than the completely speed-independent procedure in all situations, but still shows some advantages over the speed-based operational procedure at the current traffic demand. Another important and interesting finding is that the speed-based operational procedure shows more stable performance and less fuel consumption than other two procedures in the routine flying with the increase of traffic volume, while the other two have more flexibility in adjusting aircraft flying time and delay which are more suitable for air traffic flow contingency management and trajectory management.

The proposed dynamic stochastic simulation modeling framework can result in a comprehensive assessment of alternative distributed self-separation operations for air traffic in flow corridors with both realistic and simulated data. Further analysis may include different distribution of aircraft types, arrival interval, and wind disturbance etc. Also, the traffic flow management and/or trajectory management in the flow corridor would also be an interesting research direction.

This simulation modeling approach is in alignment with the NextGen and SESAR programs and, in particular, with the concepts of Trajectory-based Operations (TBO) and Self-separation (SSEP). The simulation results can also be applied in other places like the highly operated area in central Europe, and the crossing of multiple air flows had been proposed by some researchers. It also complements other initiatives that aim at improving future Air Traffic Flow Management (ATFM) across the network, such as the flow contingency management and trajectory management.

REFERENCES

[1] *NextGen Implementation Plan-FAA*, Federal Aviation Admin., Washington, DC, USA, 2017.
[2] *Guidance material for SESAR Deployment Programme Implementation*, Eur. Org. Saf. Air Navigation, France, 2018.
[3] Joint Planning and Development Office, "Concept of operations for the next generation air transportation system," Federal Aviation Admin., Washington, DC, USA, Tech. Rep. 0704-0188, Sep. 2010.
[4] A. Yousefi and A. N. Zadeh, "Dynamic allocation and benefit assessment of NextGen flow corridors," *Transp. Res. C, Emerg. Technol.*, vol. 33, pp. 297–310, Aug. 2013.
[5] J. Alipio, P. Castro, H. Kaing, N. Shahid, O. Sherzai, G. L. Donohue, and K. Grundmann, "Dynamic airspace super sectors (DASS) as high-density highways in the sky for a new US air traffic management system," in *Proc. IEEE Syst. Inf. Eng. Design Symp.*, Apr. 2003, pp. 57–66.
[6] A. Yousefi, G. Donohue, and L. Sherry, "High-volume tube-shape sectors (HTS): A network of high capacity ribbons connecting congested city pairs," in *Proc. 23rd Digit. Avionics Syst. Conf.*, Oct. 2004, pp. 3.C.1-1–3.C.1-7.
[7] H. Hering, "Air traffic freeway system for Europe," EUROCONTROL Exp. Centre, Cedex, France, Tech. Rep. 20/05, Nov. 2005.
[8] R. Hoffman and J. Prete, "Principles of airspace tube design for dynamic airspace configuration," in *Proc. 8th AIAA-ATIO Conf.*, Sep. 2008, p. 8939.
[9] G. Gupta, B. Sridhar, and A. Mukherjee, "Freeways in the sky: Exploring tube airspace design through mixed integer programming," in *Proc. INFORMS Annu. Meeting*, Washington, DC, USA, 2008, p. 6824.
[10] A. D. Mundra and E. M. Simmons, "Self-separation corridors," in *Proc. IEEE/AIAA 26th Digit. Avionics Syst. Conf.*, Dallas, TX, USA, Oct. 2007, pp. 3.C.3-1–3.C.3-11.
[11] D. J. Wing, J. C. Smith, and M. G. Ballin, "Analysis of a dynamic multi-track airway concept for air traffic management," Langley Res. Center, Hampton, VA, USA, Tech. Rep. NASA/TP-2008-215323, 2008.
[12] B. Sridhar, S. Grabbe, K. Sheth, and K. Bilimoria, "Initial study of tube networks for flexible airspace utilization," in *Proc. AIAA Guid. Navigation Control Conf.*, Aug. 2006, p. 6768.
[13] B. Sridhar, T. Islam, and G. Gupta, "Design and simulation methodology to improve the performance of airspace tube networks," in *Proc. AIAA Guid., Navigation, Control Conf.*, 2010, p. 8288.
[14] K. S. Sheth, T. S. Islam, and P. H. Kopardekar, "Analysis of airspace tube structures," in *Proc. IEEE/AIAA 27th Digit. Avionics Syst. Conf.*, Oct. 2008, pp. 3.C.2-1–3.C.2-10.
[15] M. Xue and P. H. Kopardekar, "High-capacity tube network design using the Hough transform," *J. Guid., Control, Dyn.*, vol. 32, no. 3, pp. 788–795, 2009.
[16] P. Kotecha and I. Hwang, "Optimization based tube network design for the next generation air transportation system (NextGen)," in *Proc. AIAA Guid., Navigation, Control Conf.*, 2009, p. 5860.
[17] M. Xue, "Design analysis of corridors-in-the-sky," in *Proc. AIAA Guid., Navigation, Control Conf.* Reston, VA, USA: AIAA, 2009, p. 5859.
[18] M. Xue and S. Zelinski, "Complexity analysis of traffic in corridors-in-the-sky," in *Proc. 10th Aviation Technol., Integr., Oper. Conf.*, Sep. 2010, p. 9112.
[19] B. Ye, M. Hu, and J. F. Shortle, "Collision risk-capacity tradeoff analysis of an en-route corridor model," *Chin. J. Aeronaut.*, vol. 27, no. 1, pp. 124–135, 2014.
[20] B. Ye, J. Shortle, W. Ochieng, and Y. Tian, "Sensitivity analysis of potential capacity and safety of flow corridor to self-separation parameters," *Aeronaut. J.*, vol. 123, no. 1259, pp. 56–78, 2018.
[21] Y. Zhang, J. Shortle, and L. Sherry, "Methodology for collision risk assessment of an airspace flow corridor concept," *Rel. Eng. Syst. Saf.*, vol. 142, pp. 444–455, Oct. 2015.
[22] *2013–2028 Global Air Navigation Plan-ICAO*, document 9750-AN/963, International Civil Aviation Organization, Montreal, QC, Canada, 2013.
[23] N. Takeichi, Y. Nakamura, and K. Fukuoka, "Fundamental characteristics of decentralized air traffic flow control in high density corridor," in *Proc. 28th Int. Congr. Aeronaut. Sci.*, 2012, pp. 1–9.
[24] Y. Nakamura, N. Takeichi, and K. Fukuoka, "A self-separation algorithm using speed control for width-limited high density air corridor," in *Proc. 29th Congr. Int. Council Aeronaut. Sci.*, 2014, pp. 1–10.
[25] W. Glover and J. Lygeros, *A Multi-Aircraft Model for Conflict Detection and Resolution Algorithm Evaluation*, document IST-2001-32460 of European Commission, Deliverable D1.3. European Commission, Feb. 2004.
[26] "User manual for the base of aircraft data (BADA) revision 3.8," EUROCONTROL Exp. Centre, Brétigny-sur-Orge, France, Tech. Rec. EEC Note no. 11/06, Jul. 2011.

YONG TIAN (M'17) was born in Honghu, China, in 1976. He received the Ph.D. degree in transportation planning and management from the Nanjing University of Aeronautics and Astronautics, in 2009, where he started working as an Associate Professor, in 2000. His research interests include air traffic management and airspace planning.

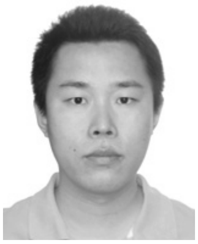

YUNLONG DONG was born in Cangzhou, China, in 1982. He is currently pursuing the Ph.D. degree in transportation planning and management with the Nanjing University of Aeronautics and Astronautics. He joined East China Air Traffic Management Bureau of Civil Aviation Administration of China, in 2007. His research interests include air traffic management and airspace planning.

BOJIA YE was born in Nanjing, China, in 1983. He received the Ph.D. degree in transportation planning and management from the Nanjing University of Aeronautics and Astronautics, in 2013, where he started working as a Lecturer, in 2013. His research interests include air traffic management and artificial intelligence.

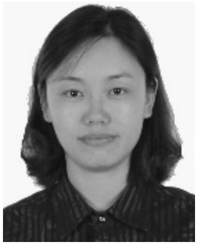

LILI WAN was born in Dongtai, China, in 1981. She received the Ph.D. degree in transportation planning and management from the Nanjing University of Aeronautics and Astronautics, in 2016, where she started working as a Lecturer, in 2005. Her research interests include air traffic management and airspace planning.